

WtE efficiency improvements: integration with solar thermal energy

L. Lombardi^{1*}, E. Carnevale² and B. Mendecka²

¹Niccolò Cusano University, Rome, via don Carlo Gnocchi 3, 00166 Italy

²Industrial Engineering Department, University of Florence, Florence, via Santa Marta 3, 50139 Italy

Abstract

Purpose. In this work energy analysis, preliminary economic evaluation and parametric study were carried out for the integration of a traditional Waste-to-Energy (WtE) plant with a concentrated solar thermal (CSP) plant, by superheating the steam produced by the WtE flue gas boiler in the solar facility.

Methods. The WtE process was simulated by a home developed thermodynamic model, which the CSP section was added to (using Engineering Equation Solver, F-Chart Software). The model requires as input the specific waste chemical composition and mass flow rate.

Results. As an example of the obtained results, it is reported here the case of using the CSP to superheat the steam exiting from the WtE evaporator. The original WtE plant – i.e. base case before introducing the integration with CSP - has a thermal power input of 50 MW and operates with superheated steam at 40 bar and 400 °C, without re-heating, condenser pressure 0.09 bar, steam turbine isentropic efficiency 0.78, 6.5% volumetric content of oxygen in the flue gas, combustion temperature equal to 1000 °C, temperature at the boiler exit 135 °C. In the stand-alone case, the WtE net output power is 11 121 kW, and the efficiency is equal to 0.22. In the integrated case, for the increasing process design parameters, of course both the net efficiency and net power output are improved, but the required CSP plant surface increased from 57 500 m² (T= 400°C, p=51 bar) to about 112 000 m² (T= 520°C, p=130 bar) in the average irradiance conditions. The specific investment cost of the integrated power plant varied from 7 697 €/kW_{net} to 10 040 €/kW_{net} compared to the 9 500€/kW_{net} for the stand alone WtE unit.

Conclusions. In general, we can conclude that CSP technology holds significant promise for extending and developing of the WtE systems. It is believed that the present results justify a further in-depth analysis.

Keywords: waste-to-energy, concentrated solar plant, efficiency.

1 Introduction

Natural resources depletion is an issue that arose to public concern in last decades and emphasized the need to transition from a linear to a circular flow of resources in the economy. European strategy for waste management attributes primary importance to waste production prevention: if less waste is generated fewer resources are consumed. Energy recovery, mainly through waste thermal treatment, is a fundamental part of the integrated waste management system, especially when related to municipal solid waste (MSW) management, for which the material recovery priority must be accomplished up-stream through separate collection system. Unsorted residual waste (i.e. the waste left downstream of separate collection) in Europe has a Lower Heating Value (LHV) of 10.3 GJ/Mg [1] and can be recovered in modern Waste-to-Energy (WtE) plants.

Nowadays, the dominant technology in WtE is incineration with energy recovery in a steam cycle. WtE plants produce energy by recovering the heat contained in the combustion gasses, through heat exchangers producing steam and they can operate producing only power, only heat or in cogeneration mode. This last possibility is pinpointed as the best techniques for energy recovery from waste [2]. However, in some cases, heat recovery is not technically feasible – due to the absence of thermal user (industrial plant or district heating) in the proximity of the WtE plant - and only power production remains as the unique possibility. In these cases, some challenges are posed in order to increase as much as possible the energy performances: high values are obtainable only for large WtE plants [3,4].

* corresponding author, lidia.lombardi@unicusano.it, tel. +393666381000

It is possible to summarize that large scale WtE plants may reach up to 30-31% net electric efficiency, in only power mode, as a maximum, while small-medium size incineration plants generally operate with steam at 40-50 bar and 400 °C, with maximum net electric efficiency around 20-24% [5].

High energy recovery efficiency values are crucial also for the environmental sustainability of WtE plants. The highest the electricity and heat produced, the best saving of natural resources may be achieved. Pavlas et al. [3] evaluated the benefits of energy recovery in WtE by CHP applying a method based on Primary Energy Saving (PES) and concluded that increase of net electrical efficiency above the 20% for medium sized units processing 100 kt/year is problematic and constrained with increasing investment costs.

The WtE energy performances are directly linked to the technological level of the designed steam cycle, mainly meaning the maximum steam pressure and temperature and complex cycle arrangements. For the steam cycle, efficiency increases as the pressure and temperature of the superheated steam increase. However, the heat transfer surfaces of WtE boilers must face severe, high temperature, acidic corrosion, caused by both the metal chlorides in the fly ash and the high concentration of hydrogen chloride (HCl) in the flue gas [6,7]. The effectiveness of high-temperature acidic corrosion depends mainly on the temperature of the metallic surface. The corrosion rate increases with temperature, hence, to limit corrosion, the temperature of the surfaces must be limited. This consideration applies both to evaporating and superheating surfaces, setting direct limits both to evaporating pressure (i.e. temperature) and superheating temperature. Flue gas temperature, at the superheater, not exceeding 650 °C, can prevent high corrosion rates [8]. Typical superheated steam pressure and temperature are 40 bars and 400°C, even if recently built WtE plants operate with increased values of pressure and temperature up to, respectively, 60 bars and 500 °C [5].

To cope with these technical constraints, alternative configurations were proposed. As an example, superheating of live steam from 400 °C to 520 °C in an external superheater, consisting of natural gas fired boiler, was realized in a new WtE plant in Heringen (Germany) [9]. The possibility of integrating WtE with combined steam–gas cycle was proposed and studied, basing on the idea of superheating the steam produced by the WtE flue gas boiler using cleaner exhausts, as for example gas turbine exhausts, in order to allow raising the superheated steam temperature, without the above-mentioned corrosion risks [10–14].

Steam superheating may also be realized by integration of a concentrated solar power (CSP) subsystem into the WtE plant. With increasing concerns on CO₂ emission, such a concept may become a promising and competitive technology and contribute significantly to the EU2020 goals achievement, especially for regions with high direct normal irradiance (DNI).

At present, four CSP technologies are commercially available [15]: parabolic trough collector (PTC), solar power tower (SPT), linear Fresnel reflector (LFR) and parabolic dish systems (PDS). Solar power towers (SPT), also known as central receiver systems (CRS), use a heliostat field collector (HFC), i.e., a field of sun-tracking reflectors, called heliostats, that reflect and concentrate the sun rays onto a central receiver placed on the top of a fixed tower.

The possibility of integration of solar energy into conventional power cycles has been successfully demonstrated in numerous studies. The majority of these works focused on the integration of solar power with natural gas combined cycle (NGCC) [16–20] or conventional coal-fired power generation system [21–23]. Zhu et al. [16] proved the overall NGCC plant efficiency is noticeably (from 34 to 44%) boosted with the solar addition. As another example, Franchini et al. [18] compared the thermodynamic performance of PTC and SPT technologies in direct Rankine Cycle and integrated solar – NGCC plants. Results showed that the hybrid SPT-NGCC yielded the highest solar-to-electric efficiency.

Currently, the number of scientific studies focusing on hybrid CSP-biomass systems is also increasing [24–26]. In general, the studies conclude that for the favorable ambient conditions, overall energy efficiencies of the power plants can be significantly improved through the solar integration.

Combining WtE plants with solar energy is not entirely new concept. However, not so many relevant studies can be found in the literature.

In this work, we propose to integrate a traditional WtE with a concentrated solar power (CSP) plant, by superheating the steam produced by the WtE flue gas boiler in the SPT solar facility. The work presented in the following paragraphs and the related results are to be indented as preliminary evaluations, while developments are presently ongoing. As a matter of fact, the aim of the present work is the preliminary coupling of the WtE and CSP plants, in order to supply a first evaluation of the energy performance increase and a draft calculation of the additional investment cost for the CSP with respect to the WtE. The main questions the authors would like to answer at this stage are: how much the CSP integration will influence the thermodynamic performance and overall plant cost.

2 Materials and methods

Since the objective of the paper is to provide a preliminary thermodynamic and economic evaluation of the system, the proposed case study is a simplified structure operating at nominal parameters, yet correctly representing the transformations of energy in subsequent devices. Operational problems like part-load characteristics, non-steady operation with heat storage, the temporal distribution of demand and control strategies, etc. are not discussed.

The schematic diagram of the considered WtE+CSP model is presented in Fig. 1. The WtE system is based on integrated boiler grid furnace (B) fueled by MSW. In the solar cycle, molten salts mixture is considered as the working fluid in the solar receiver (SC). The solar field is composed of heliostats (H), which reflect and concentrate sun radiation on a receptor (R) located on the upper part of a solar tower. In the simplified case, molten salt is pumped from a cold storage tank (CST) through the receiver, where it is heated, and then stored in the hot tank (HST). Heat generated in the solar cycle is then transferred to the bottoming WtE cycle, by means of the heat exchanger (SH). Hot salt is pumped to a heat exchanger where the steam is superheated, and the exiting salt is returned to the cold tank where it is stored. Superheated steam feeds the high-pressure steam turbine (STHP). Usable products of the cycle comprise electricity (net power output). Heat production is not considered in this study.

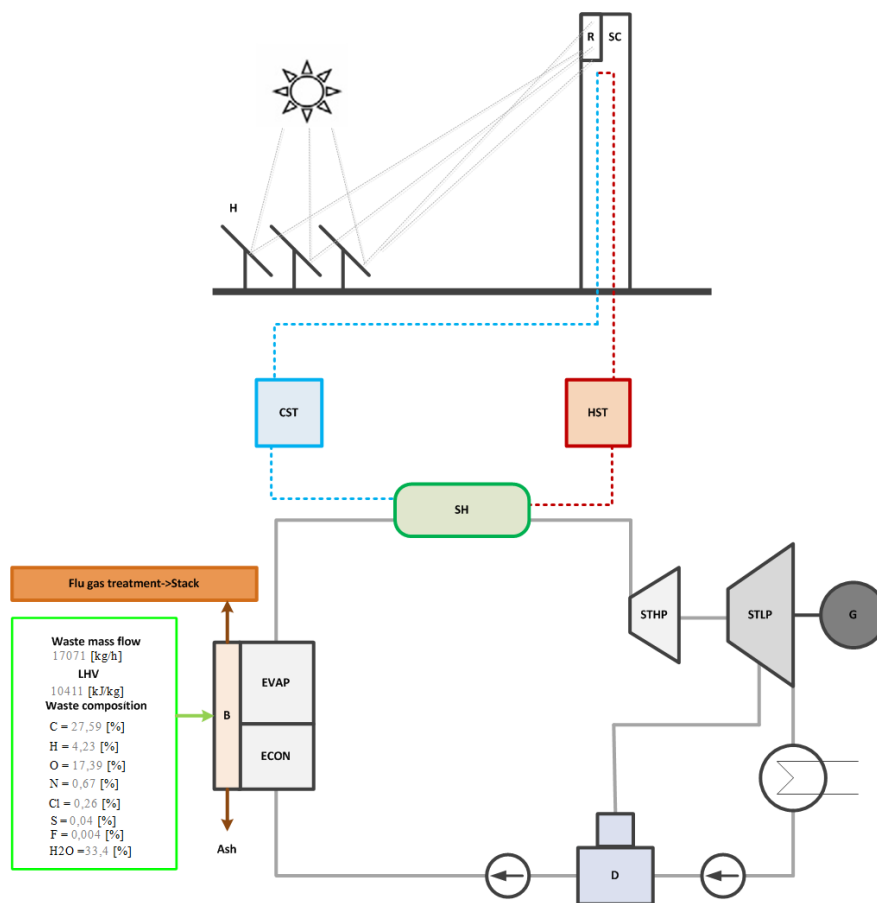


Fig.1 Schematic diagram of analyzed WtE+CSP plant.

2.1 WtE simulation

Conventional steady-state mass balances (involving stoichiometry) and energy balances for the WtE part were resolved by a home developed thermodynamic model (using Engineering Equation Solver, F-Chart Software). The model requires as input the specific waste chemical composition and mass flow rate. Complete combustion of the entering waste is assumed with the exception of part of the solid carbon, equivalent to 3% in mass of the bottom ash (BA). The energy balance in the combustion chamber is performed assuming an integrated boiler grid furnace, assigning the volumetric content of oxygen, combustion temperature, and heat losses. The combustion gas mass flow rate is calculated and used, in turn, to calculate the steam mass flow rate produced in the boiler, assuming the assigned levels of pressure and temperature for the superheated/saturated steam. The total in-plant specific consumption was assumed to be equal to 105 kWh per Mg of waste [1].

The code was used to simulate the base case of a stand-alone WtE, producing superheated steam expanding in the steam turbine, according to the specifications reported in Table 1.

Table 1. Main assumption and design parameters for the WtE simulation.

Thermal power input - plant size [MW]	50
MSW throughput [Mg/y]	135 199
MSW LHV	10.5
Steam maximum pressure [bar]	40
Steam maximum temperature [°C]	400
Steam mass flow [Mg/h]	54.3
O ₂ in the flue gas at the boiler exit [% vol.]	6.5
Flue gas temperature at the stack [°C]	135
Turbine isentropic efficiency	0.78
Gross power output [MW]	12.6
Self-consumption rate, %	13.8
Net electrical efficiency	0.22

2.2 CSP simulation

The CSP section model was added into the same code. When the CSP is integrated into the system, the WtE plant boiler is used to produce only saturated steam at the design pressure. Consequently, the saturated steam mass flow rate generated in this operation mode is higher than the corresponding stand-alone WtE operation mode. The CSP section is sized on the basis of the mass flow rate of saturated steam produced in the WtE section. Design parameters of the solar part were taken from the Gemasolar study case [27–29]. These include, for example, the area of the single heliostat (120m²) and the size of the storage tanks. Moreover, a mixture of molten salts (60% NaNO₃ and 40% by KNO₃) was considered as a heat transfer fluid (HTF) in the solar tower. Such an HTF is the most commonly used mixture in CSP plants, thanks to the low cost (many fertilizers have the same composition) and excellent thermodynamic properties [30]. The chosen HTF has a usable temperature range of 290-565 °C [31], and this range was set as a limit in the CSP model. The pinch point temperature difference between the temperature of the steam exiting the evaporator and the temperature of hot HTF was previously set as 25°C. The specific heat and density of HTF were calculated using the following relations [30,32]:

$$c_p = 1443 + 0.172 \cdot T \quad \left[\frac{J}{kg \cdot ^\circ C} \right] \quad (1)$$

$$\rho = 2090 - 0.636 \cdot T \quad \left[\frac{kg}{m^3} \right] \quad (2)$$

The data considered for heliostat field efficiencies were adapted from the literature and are presented in Table 2.

Table 2. Main assumption and design parameters for the heliostat field [31].

Solar Multiple	2
Cosine efficiency	0.94
Shading and blocking factor	0.75
Interception of sun rays at the aperture	0.90
Atmospheric attenuation	0.90
Heliostat reflectivity	0.90
Overall heliostat efficiency	0.52

2.3 Simulation conditions

The integration of WtE-CSP plant was simulated varying the superheated steam parameters. Temperature ranged between 400°C and 520 °C. The upper limit is imposed by the maximum temperature allowable for the molten salts, which cannot be higher than 565 °C (a temperature difference was obviously kept). Pressure ranged between 51 and 120 bars. The lower limit is imposed by the minimum temperature imposed for the salts, since they solidify at 290 °C, assuming a temperature difference between the temperature of the salts and the saturated steam one of 25 °C. Parametric simulation was also performed under different nominal DNI values ranging from 500 to 1000 W/m².

2.4 Assumptions for the preliminary evaluation of the investment costs

A preliminary economic analysis has been carried out to evaluate the specific investment costs of the WtE+CSP plant working under different conditions. The economic investment cost model is based on exponential relations proposed previously by Bejan et al. and Petersen et al. [33,34]. The data on the total investment cost of a reference stand-alone WtE were assumed on the basis of the total plant cost of about 59 MW WtE plant operating In Italy.

The investment cost of the WtE plant under varying the superheated steam parameters was calculated using the following relation (3):

$$C_{WtE} = C_{fix,WtE} + \left(0.1 \times C_{th,WtE} + 0.9 \times C_{th,WtE} \left(\frac{m_{vap}}{m_{vap,ref}} \right)^{0.7} \right) \quad (3)$$

Where $C_{fix,WtE}$ refers to the fuel supply system, ash handling system, water supply and treatment system, electrical system, automatic and control system. These parts of the WtE plant are here assumed, as independent on the steam cycle parameters, fixed values. The contribution of the fixed part was assumed as 38% [35]. The cost of thermal part of the WtE – i.e. mainly boiler and steam cycle – was assumed to change according to the change in the generated steam mass flow rate. The cost exponent was assumed equal to 0.7 as the average value for the electric power plants following Bejan et al. [33].

The cost of the solar part has been evaluated using the data collected from literature: all the parameters and data used in the economic analysis are summarized in Table 3.

Table 3. Main assumptions for the economic analysis.

Investment cost of reference WtE unit, mln€	111 774
Specific cost of reference WtE unit, €/kW _{LHV}	1 899
Specific cost of reference WtE unit, €/kW _{net}	9 503
Specific cost of solar field, €/m ²	200*
Specific cost of thermal storage system, €/kWh	30*
Specific cost of tower and receiver, €/MW	200*

*[36]

3 Results

In this paragraph results of the thermodynamic analysis are first reported. Then the results of the estimation of investment cost are illustrated.

3.1 Thermodynamic analysis results

Selected results of the thermodynamic parametric study for DNI=600 W/m² are presented in Fig. 2, 4, 6 and 8. The influence of different DNI values (from 500-1000 W/m²) is presented in Fig. 3,5,7 and 9.

Figs.2 and 3 shows the variation of the net power output under different process design parameters and different DNI. the parameters such as power output or electrical efficiency will be obviously affected by the process design parameters. Firstly, it can be observed that the power output increases significantly for the higher steam parameters. In particular, the increase from 15.7 MW_{gross} to 20.3 MW_{gross}, compared to the 12.6 MW_{gross} obtained in the stand-alone WtE plant is noted. On the contrary, the power output is not affected by the different DNI conditions as can be seen in Fig. 3. As a matter of fact, the code calculates the saturated steam mass flow rate that can be produced at the design pressure in the WtE, then in the solar section the thermal power required for superheating this steam mass flow rate, at the design temperature, is calculated. In the case of different DNI

values, the required thermal power remains the same, but obviously, a larger heliostat surface is required. The steam cycle gross power output, consequently, is not affected.

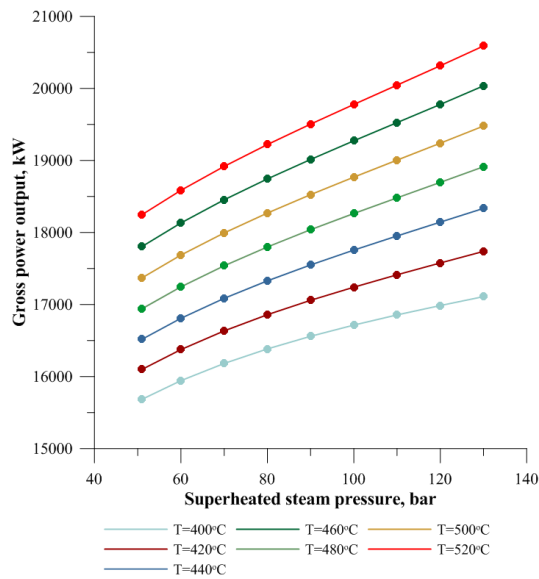


Fig.2 Gross power output as a function of temperature and pressure of superheated steam (DNI=600 W/m²).

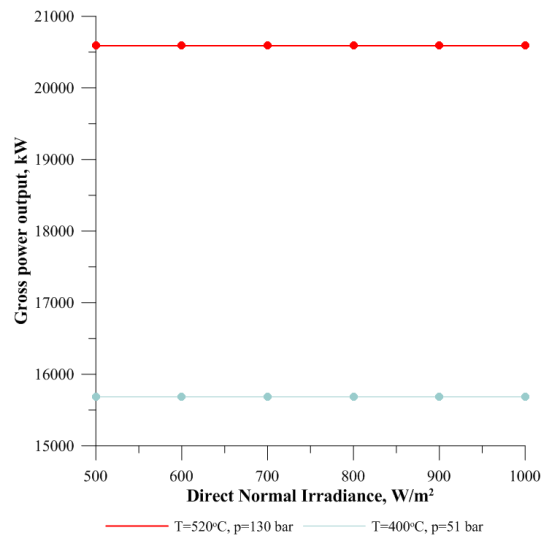


Fig.3 Gross power output as a function of direct normal irradiance.

Later, it is observed (Fig.4 and 5) the decrease of about 2% of the self-consumption rate with the increase of process design parameters. As a contrast to the previous results, self-consumption rate is affected by the different irradiance condition, because the electrical consumptions for heliostat control systems change with their overall surface. Depending on the DNI conditions, the self-consumption rate varies from 10.2-11.5% and from 12.4-13.3% for the higher (T= 520°C, p=130 bar) and lower (T= 400°C, p=51 bar) process parameters, respectively. The obtained values are lower than for the ones regarding the WtE stand-alone plant (13.8%), being increased the gross power output.

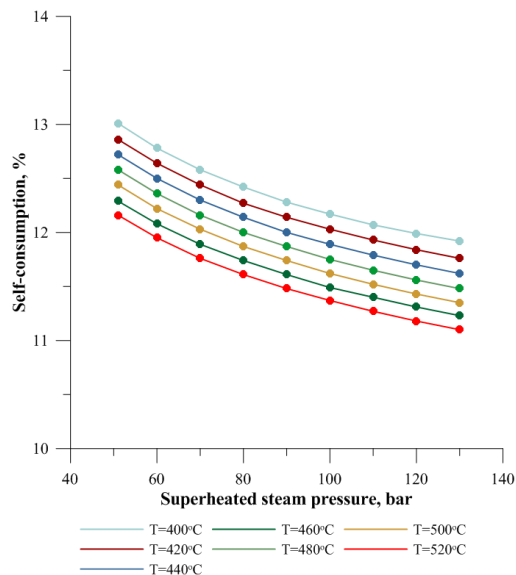


Fig.4 Self-consumption rate as a function of temperature and pressure of superheated steam (DNI=600 W/m²)

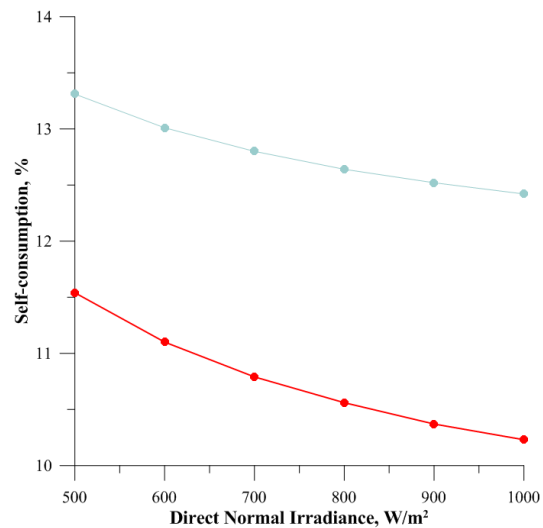


Fig.5 Self-consumption rate as a function of direct normal irradiance

The net electric efficiency's behavior is similar to the power output's one. For the increasing steam design parameters, the increase of net electric efficiency is observable. The addition of solar power affects the net

electrical efficiency performance with respect to the stand-alone WtE plant. In particular the net electric efficiency passed from the 0.22 to 0.290 and 0.238, respectively for the higher ($T= 520^{\circ}\text{C}$, $p=130$ bar) and lower ($T= 400^{\circ}\text{C}$, $p=51$ bar) process parameters, respectively.

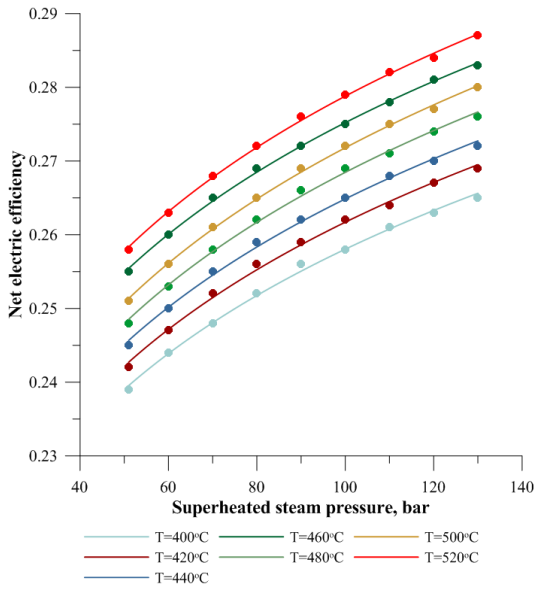


Fig.6 Net electrical efficiency as a function of temperature and pressure of superheated steam ($\text{DNI}=600 \text{ W/m}^2$).

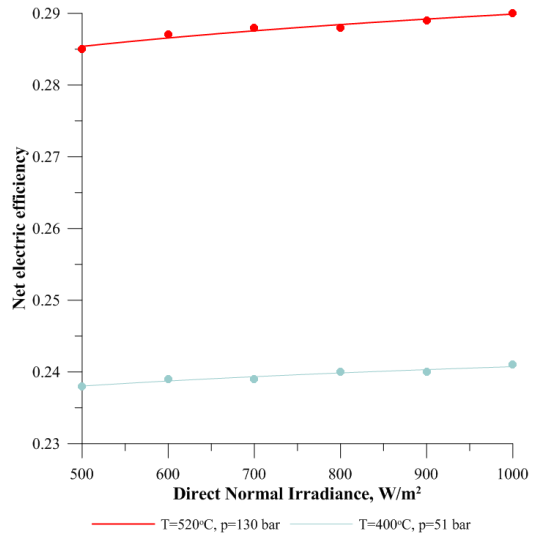


Fig.7 Net electrical efficiency as a function of direct normal irradiance.

In general, the thermodynamic parametric analysis shows the energy profits can be achieved by increasing the process design parameters. Increasing the steam parameters should also be justified by the economic analysis.

3.2 Preliminary evaluation of the investment costs

In the following section, the initial results of the investment cost analysis are presented. As can be observed in Fig. 8, the investment cost of WtE power plant increases significantly, with the higher steam pressure conditions. Working at the increased pressure operation mode, the higher steam mass flow rate is produced and consequently, the larger size of the thermal section is required. The cost of the thermal part is not affected by the different irradiance conditions as can be seen in Fig. 9. Assuming the lowest values of the analyzed steam parameters ($T=400^{\circ}\text{C}$, $p=51$ bar), the investment cost of WtE part of the integrated cycle is about 7% higher compared to the stand-alone WtE plant. Such an investment allows to obtain, depending on the DNI, from 2.0 to 5.0 percentage point growth of net electric efficiency.

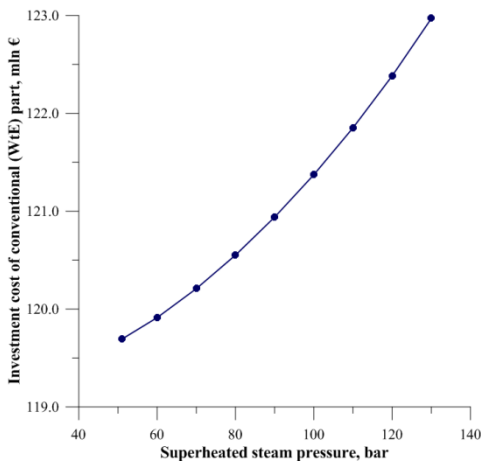


Fig.8 Investment cost of WtE part as a function of temperature and pressure of superheated steam. ($\text{DNI}=600 \text{ W/m}^2$).

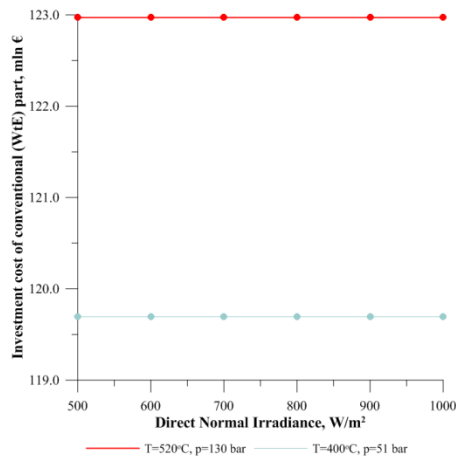


Fig.9 Investment cost of WtE part as a function of direct normal irradiance (DNI).

For the further comparison, the total investment cost including the solar part should be taken into account. The major contributor to the investment cost of the solar part of the power cycle is heliostat field and the receiver. Figs.10 and 11 present the influence of the different steam parameters and different DNI on the entire heliostat field. The area of the heliostat field required to produce sufficient amount of heat for the steam superheating increases with the both steam temperature and pressure. It can also be observed strong dependency of the heliostat field area and the irradiance conditions, notably for the higher steam temperature and pressure, where the heliostat area decreases more significantly. Comparing the results from Fig. 10 and Fig.11, it can be seen that, for the sites with DNI higher than 900 W/m^2 , it is possible to achieve the heliostat size, below $75\,000 \text{ m}^2$, similar to one for the lower steam parameters ($T=460^\circ\text{C}$, $p=90 \text{ bar}$) and DNI (600 W/m^2).

Considering the minimum and maximum process design parameters case, for the 1000 W/m^2 DNI conditions, almost two times larger field is required to achieve the maximum steam parameters and thus to increase the net electrical efficiency from 0.238 to 0.290 (Fig. 7). Similar tendencies are observed for the total investment cost of the solar part (Fig. 14 and 15).

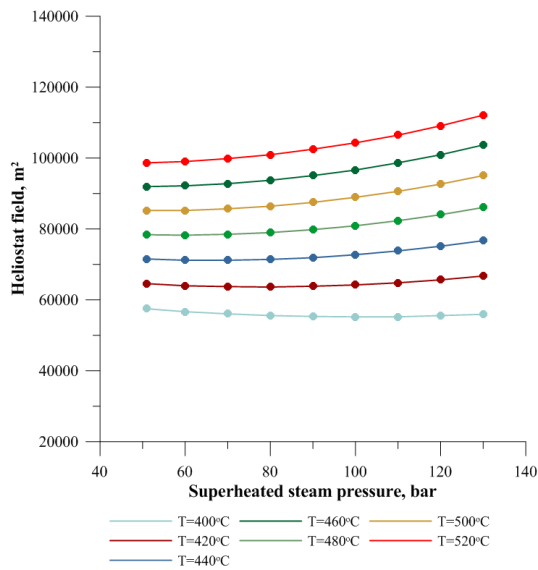


Fig.10 Heliostat field as a function of temperature and pressure of superheated steam ($\text{DNI}=600 \text{ W/m}^2$).

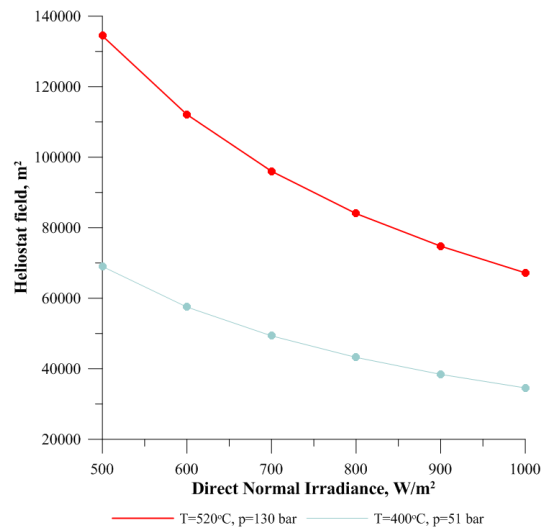


Fig.11 Heliostat field as a function of direct normal irradiance (DNI).

Salt mass flow, which affects the receiver power, increases with the higher process design requirements (Fig. 12) but remain the same for the different DNI conditions (Fig.13).

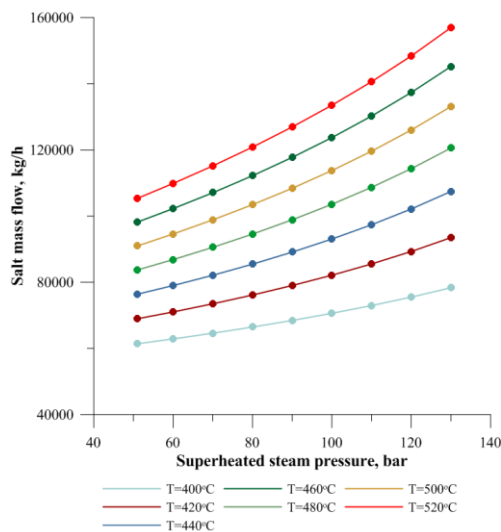


Fig.12 Molten salt mass flow as a function of temperature and pressure of superheated steam ($\text{DNI}=600 \text{ W/m}^2$).

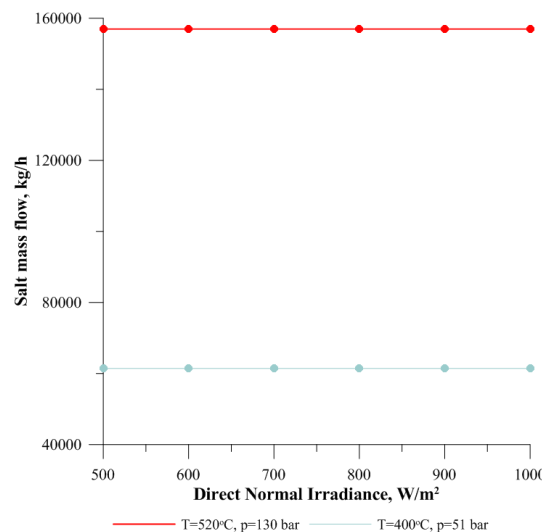


Fig. 13. Molten salt mass flow as a function of direct normal irradiance (DNI).

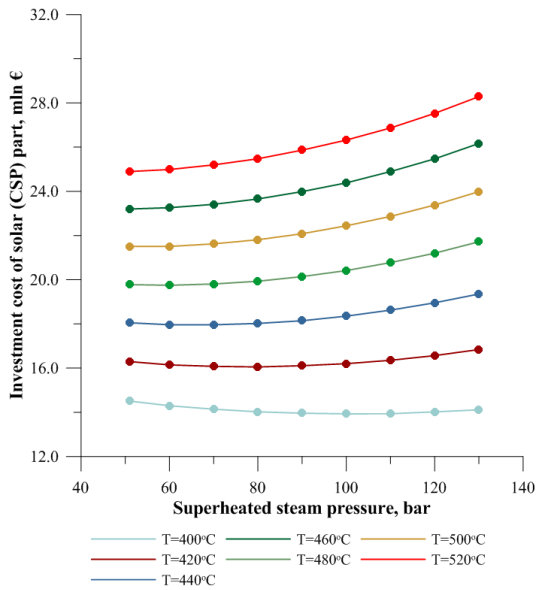


Fig.14 Investment cost of solar part as a function of temperature and pressure of superheated steam (DNI=600 W/m²).

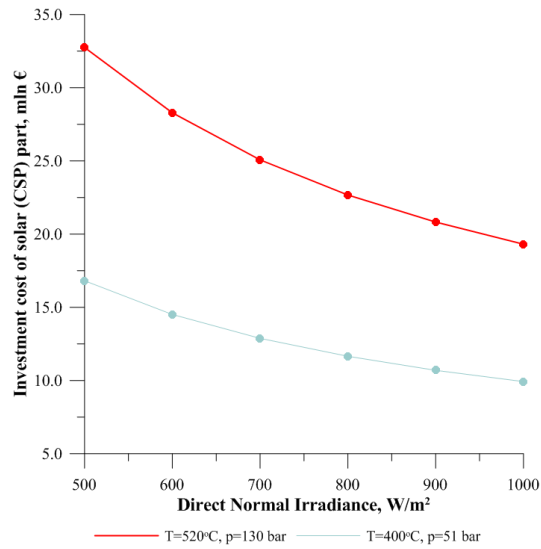


Fig.15 Investment cost of solar part as a function of direct normal irradiance (DNI).

Figs. 16 and 17 present the variation of the specific cost of the WtE+CSP plant in reference to the net power output. As can be observed, the specific cost decreases noticeable for the higher steam parameters and for the more favorable DNI. For the lowest DNI, the cost contribution of the solar part of the power plant varies from 14 to 26 % to the total cost. For the nominal solar irradiance of 1000 W/m², the contribution is lower reaching from 8-13% depending on the process design parameters.

What is interesting, even if the solar part contributes noticeably to the total cost of the power plant, the specific investment cost of the net power output generated in the stand-alone WtE plant in majority cases is higher than of total specific cost for the solar integrated power plant. As can be seen, from Fig. 16, assuming average DNI conditions, and the lowest steam temperature, the specific cost of WtE+CSP plant is higher only below the steam pressure of 70 bars. Nevertheless, also the integrated WtE+CSP plant working on the lowest analyzed steam parameters may be economically viable, when the nominal solar conditions are high (more than 900 W/m² – Fig. 17).

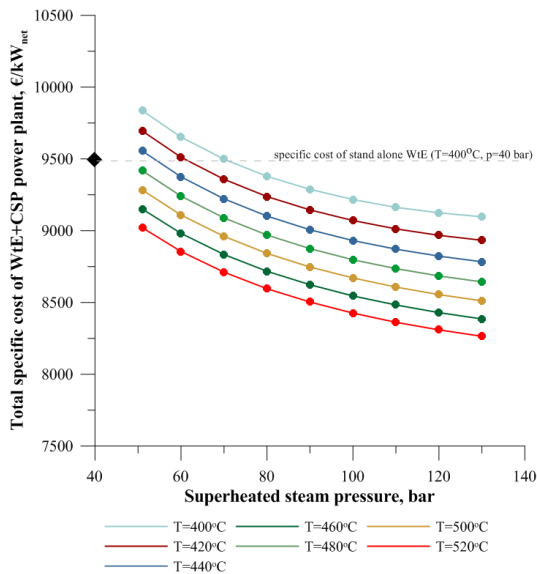


Fig.16 Specific cost of WtE+CSP plant as a function of temperature and pressure of superheated steam (DNI=600 W/m²).

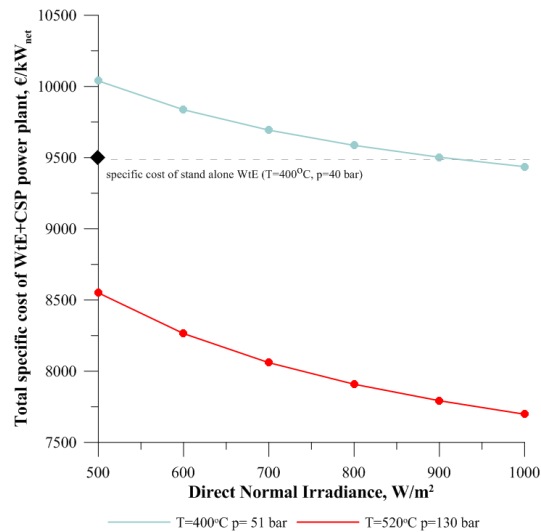


Fig.17 Specific cost of WtE+CSP plant as a function of direct normal irradiance.

4 Conclusions

The study proposes and preliminarily investigates the thermodynamic and economic performance of the integrated system of the WtE steam cycle coupled with a solar tower, where steam superheating takes place.

The influence of the temperature, pressure and direct solar irradiance on the energy and economic effects have been studied. Compared to the stand-alone WtE cycle, the integrated WtE+CSP can achieve from 2 to 5 better efficiency points, for the lowest process design parameters depending on the DNI conditions. The preliminary economic evaluation shows that the solar part of the plant increases the total investment cost significantly. However, the increase obtained in the net power production can economically justify the proposed integration.

In general, we can conclude that CSP technology holds significant promise for extending and developing of the WtE systems. It is believed that the present results justify an in-depth analysis. For the further improvements, the model needs to be developed in order to optimize the process and to allow to perform the dynamic analysis of the CSP section, including the trends of the solar radiation, and consequently the complete economic analysis. Moreover, even if the preliminary economic analysis revealed the viability of the solar power implementation to the WtE, the system should be evaluated from the environmental profits point of view.

5 References

- [1] Reimann, D. O., 2012. CEWEP Energy Report III. (Status 2007-2010).
- [2] European Commission, 2006. Reference Document on the Best Available Techniques for Waste Incineration. n.d.
- [3] Pavlas M, Touš M, Klimek P, Bébar L. Waste incineration with production of clean and reliable energy. *Clean Technol Environ Policy* 2011;13:595–605. doi:10.1007/s10098-011-0353-5.
- [4] Consonni S, Viganò F. Waste gasification vs. conventional Waste-To-Energy: A comparative evaluation of two commercial technologies. *Waste Manag* 2012;32:653–66. doi:10.1016/j.wasman.2011.12.019.
- [5] Lombardi L, Carnevale E, Corti A. A review of technologies and performances of thermal treatment systems for energy recovery from waste. *Waste Manag* 2015;37:26–44. doi:10.1016/j.wasman.2014.11.010.
- [6] Lee S-H, Themelis NJ, Castaldi MJ. High-Temperature Corrosion in Waste-to-Energy Boilers. *J Therm Spray Technol* 2007;16:104–10. doi:10.1007/s11666-006-9005-4.
- [7] Persson K, Broström M, Carlsson J, Nordin A, Backman R. High temperature corrosion in a 65 MW waste to energy plant. *Fuel Process Technol* 2007;88:1178–82. doi:10.1016/j.fuproc.2007.06.031.
- [8] De Greef J, Villani K, Goethals J, Van Belle H, Van Caneghem J, Vandecasteele C. Optimising energy recovery and use of chemicals, resources and materials in modern waste-to-energy plants. *Waste Manag* 2013;33:2416–24. doi:10.1016/j.wasman.2013.05.026.
- [9] Main A, Maghon T. Concepts and Experiences for Higher Plant Efficiency With Modern Advanced Boiler and Incineration Technology, ASME; 2010, p. 33–40. doi:10.1115/NAWTEC18-3541.
- [10] Consonni S, Silva P. Off-design performance of integrated waste-to-energy, combined cycle plants. *Appl Therm Eng* 2007;27:712–21. doi:10.1016/j.applthermaleng.2006.10.014.
- [11] Qiu K, Hayden ACS. Performance analysis and modeling of energy from waste combined cycles. *Appl Therm Eng* 2009;29:3049–55. doi:10.1016/j.applthermaleng.2009.04.003.
- [12] Poma C, Verda V, Consonni S. Design and performance evaluation of a waste-to-energy plant integrated with a combined cycle. *Energy* 2010;35:786–93. doi:10.1016/j.energy.2009.08.036.
- [13] Udomsri S, Martin AR, Fransson TH. Economic assessment and energy model scenarios of municipal solid waste incineration and gas turbine hybrid dual-fueled cycles in Thailand. *Waste Manag* 2010;30:1414–22. doi:10.1016/j.wasman.2010.02.009.
- [14] Balcazar JGC, Dias RA, Balestieri JAP. Analysis of hybrid waste-to-energy for medium-sized cities. *Energy* 2013;55:728–41. doi:10.1016/j.energy.2013.02.003.
- [15] Zhang HL, Baeyens J, Degreè J, Cacères G. Concentrated solar power plants: Review and design methodology. *Renew Sustain Energy Rev* 2013;22:466–81. doi:10.1016/j.rser.2013.01.032.
- [16] Zhu G, Neises T, Turchi C, Bedilion R. Thermodynamic evaluation of solar integration into a natural gas combined cycle power plant. *Renew Energy* 2015;74:815–24. doi:10.1016/j.renene.2014.08.073.
- [17] Merchán RP, Santos MJ, Reyes-Ramírez I, Medina A, Calvo Hernández A. Modeling hybrid solar gas-turbine power plants: Thermodynamic projection of annual performance and emissions. *Energy Convers Manag* 2017;134:314–26. doi:10.1016/j.enconman.2016.12.044.

- [18] Franchini G, Perdichizzi A, Ravelli S, Barigozzi G. A comparative study between parabolic trough and solar tower technologies in Solar Rankine Cycle and Integrated Solar Combined Cycle plants. *Sol Energy* 2013;98:302–14. doi:10.1016/j.solener.2013.09.033.
- [19] Manente G. High performance integrated solar combined cycles with minimum modifications to the combined cycle power plant design. *Energy Convers Manag* 2016;111:186–97. doi:10.1016/j.enconman.2015.12.079.
- [20] Alqahtani BJ, Patiño-Echeverri D. Integrated Solar Combined Cycle Power Plants: Paving the way for thermal solar. *Appl Energy* 2016;169:927–36. doi:10.1016/j.apenergy.2016.02.083.
- [21] Yang Y, Cui Y, Hou H, Guo X, Yang Z, Wang N. Research on solar aided coal-fired power generation system and performance analysis. *Sci China Ser E Technol Sci* 2008;51:1211–21. doi:10.1007/s11431-008-0172-z.
- [22] Yang Y, Yan Q, Zhai R, Kouzani A, Hu E. An efficient way to use medium-or-low temperature solar heat for power generation – integration into conventional power plant. *Appl Therm Eng* 2011;31:157–62. doi:10.1016/j.applthermaleng.2010.08.024.
- [23] Hu E, Yang Y, Nishimura A, Yilmaz F, Kouzani A. Solar thermal aided power generation. *Appl Energy* 2010;87:2881–5. doi:10.1016/j.apenergy.2009.10.025.
- [24] Liu Q, Bai Z, Wang X, Lei J, Jin H. Investigation of thermodynamic performances for two solar-biomass hybrid combined cycle power generation systems. *Energy Convers Manag* 2016;122:252–62. doi:10.1016/j.enconman.2016.05.080.
- [25] Bai Z, Liu Q, Lei J, Hong H, Jin H. New solar-biomass power generation system integrated a two-stage gasifier. *Appl Energy* 2017;194:310–9. doi:10.1016/j.apenergy.2016.06.081.
- [26] Milani R, Szklo A, Hoffmann BS. Hybridization of concentrated solar power with biomass gasification in Brazil's semiarid region. *Energy Convers Manag* 2017;143:522–37. doi:10.1016/j.enconman.2017.04.015.
- [27] Torresol Energy - Gemasolar thermosolar plant n.d. <http://www.torresolenergy.com/TORRESOL/gemasolar-plant/en> (accessed May 16, 2017).
- [28] Behar O, Khellaf A, Mohammedi K, Ait-Kaci S. A review of integrated solar combined cycle system (ISCCS) with a parabolic trough technology. *Renew Sustain Energy Rev* 2014;39:223–50. doi:10.1016/j.rser.2014.07.066.
- [29] Gemasolar, the first tower thermosolar commercial plant with molten salt storage. ResearchGate n.d. https://www.researchgate.net/publication/264855919_Gemasolar_the_first_tower_thermosolar_commercial_plant_with_molten_salt_storage (accessed May 17, 2017).
- [30] Kenisarin MM. High-temperature phase change materials for thermal energy storage. *Renew Sustain Energy Rev* 2010;14:955–70. doi:10.1016/j.rser.2009.11.011.
- [31] ENEA – Agenzia nazionale per le nuove tecnologie, l'energia e lo sviluppo economico sostenibile. Crescenzi, T., Fontanella, A., Liberatore, R., Metelli, E., Russo, V., 2013. Analisi tecnico-economica di impianti solari a collettori parabolici lineari con differenti fluidi di lavoro. Report RdS/2013/077. n.d.
- [32] Cádiz P, Frassetto M, Silva M, Martínez F, Carballo J. Shadowing and Blocking Effect Optimization for a Variable Geometry Heliostat Field. *Energy Procedia* 2015;69:60–9. doi:10.1016/j.egypro.2015.03.008.
- [33] Bejan A, Moran MJ. *Thermal Design and Optimization*. John Wiley & Sons; 1996.
- [34] Peters M, Timmerhaus K, West R. *Plant Design and Economics for Chemical Engineers*. McGraw-Hill Education; 2003.
- [35] Xin-gang Z, Gui-wu J, Ang L, Yun L. Technology, cost, a performance of waste-to-energy incineration industry in China. *Renew Sustain Energy Rev* 2016;55:115–30. doi:10.1016/j.rser.2015.10.137.
- [36] Avila-Marin AL, Fernandez-Reche J, Tellez FM. Evaluation of the potential of central receiver solar power plants: Configuration, optimization and trends. *Appl Energy* 2013;112:274–88. doi:10.1016/j.apenergy.2013.05.049.